아시아리뷰 제15권 제3호(통권 35호), 2025: 355~388 https://doi.org/10.24987/SNUACAR.2025.12.15.3.355

Sustainable Development Pathways for Plain Cities from a Multi-Model Integration Perspective: A Case Study of Chengdu

Ting Lei* Master's Student, College of Geography and Ocean Sciences, Yanbian University
Shouzhi Zhang** Associate Professor, College of Geography and Ocean Sciences, Yanbian University

Elucidating the trajectory of landscape ecological risk in Chengdu provides an empirical basis for ecological risk management within the city's jurisdiction, holding important practical value for promoting urban sustainable development. Through five periods of land use data covering the period of 2000-2020, this paper employs the landscape pattern index method to evaluate the landscape ecological risk index for the corresponding years in an effort to delineate the evolving patterns of the risk over time and space. To identify the clustered distribution of landscape ecological risk, we conducted a spatial autocorrelation analysis. Using the MOP-FLUS model, the geographical arrangement of landscape categories under four distinct 2035 scenarios is projected, enabling predictions of future landscape ecological risk trends. The findings reveal the following: (1) From 2000 to 2020, the overall landscape ecological risk in Chengdu showed a declining trend, and the risk level structure continued to optimize; (2) the landscape ecological risk index presented an overall pattern of "lower in the west and higher in the east," with low-risk areas consistently clustered in the western ecological barrier and with high-risk areas persistently concentrated in the central plains; (3) multi-scenario simulations demonstrate that Ecological-Priority Development scenario can effectively control the expansion of high-risk areas, representing the optimal pathway for maintaining regional ecological sustainability.

주제어 Landscape type, Landscape ecological risk, Multi-scenario, MOP-FLUS model

I. Introduction

The global wave of urbanization, while a cornerstone of socioeconomic development, poses unprecedented challenges to regional ecological sustainability. By 2050, nearly 70% of the world's population is projected to reside in urban areas, marking a significant transition that intensifies

* First author (1904157330@qq.com)
** Corresponding author (szzhang@ybu.edu.cn)

competition for land and triggers a range of cascading environmental issues, including landscape fragmentation, biodiversity loss, and ecosystem degradation. These pressures are particularly intense in flat regions, where topography and few natural barriers promote rapid and frequently disordered urban sprawl. Understanding and steering the sustainable development of these "plain cities"—defined here as urban entities situated predominantly on flat terrain, characterized by intensive land use, low natural resistance to spatial expansion, and high vulnerability of their intertwined agricultural and semi-natural ecosystems—is therefore a critical global imperative.

Landscape Ecological Risk (LER) assessment has emerged as a vital tool for quantifying these impacts. Simply put, LER measures the likelihood of ecosystem degradation resulting from changes in landscape patterns caused by human and natural disturbances. The widely adopted landscape pattern index method effectively translates land-use change into spatiotemporal risk patterns, making it suitable for regional-scale studies. While numerous studies have used this method to reconstruct historical LER, a significant gap remains in proactively forecasting future risk under alternative development scenarios.

Accurately predicting future LER hinges on reliably simulating land-use configurations. While foundational models like CA-Markov (Hamad et al., 2018) and CLUE-S (Luo et al., 2010) exhibit limitations in simulating complex competition among land-use types, the integrated MOP-FLUS model offers a superior framework. The FLUS model adeptly handles complex interactions in human-dominated landscapes (Liu et al., 2021), whereas Multi-Objective Programming (MOP) incorporates top-down optimization for conflicting goals such as economic growth and ecological conservation (Guo et al., 2023). This integration is particularly promising for application in plain cities, whose unique spatial dynamics—where the highest ecological risks

may not be in the dense urban core, but rather in the peri-urban fringe and along sensitive corridors—require a dedicated investigation.

To bridge these gaps, this study employs the MOP-FLUS model to explore sustainable pathways for plain cities, using Chengdu as a paradigmatic case. Chengdu, a major metropolis on the Chengdu Plain, exemplifies a plain city with its flat topography, rapid circular expansion, and intense competition among farmland, ecological, and construction land. We first assess the spatiotemporal evolution of LER from 2000 to 2020, then simulate and compare LER patterns for 2035 under four scenarios: Natural Development (ND), Economic-Priority Development (END), Ecological-Priority Development (ELD), and Coordinated Development (CD).

This research aims to provide three key contributions: (1) methodological, by demonstrating the value of the MOP-FLUS integration for balancing economic and ecological objectives; (2) empirical, by revealing the distinctive spatial signatures of LER in a typical plain city; and (3) practical, by offering actionable insights for spatial planning and ecological stabilization in Chengdu and similar urban contexts worldwide.

II. Materials and Methods

1. Study Area

The research is situated in the western Sichuan Basin of central Sichuan Province, China (102°54′-104°53′E, 30°05′-31°26′N). The region extends 192 km east-west and 166 km north-south, with a total area of 1,433,500 hm^2. Administratively, it's composed of a total of 20 divisions: 12 districts, 3 counties, and 5 county-level cities (Fig. 1). Located at the convergence zone of the western Sichuan Basin and the eastern foothills of the Qinghai-

Tibet Plateau, the study area features complex topography bordered by Ya'an and Aba to the west, and neighboring Deyang, Ziyang, and Meishan to the east. The region exhibits a distinct west-high-east-low topographic pattern. Significant altitudinal variation across the study area has formed a landform where plains, hills, and mountains each constitute approximately one-third of the territory. The climate is characterized as a subtropical monsoon type with clear seasonal variations and warm, humid conditions. The area's climate is characterized by a mean annual temperature of 16.7℃ and annual precipitation of 734.8 mm~1142.3 mm, with evenly distributed rainfall moderately concentrated during the summer Meiyu season. The Min River, revered as the cradle of civilization in the Chengdu Plain, flows through the urban area and plays a vital role in sustaining the urban water supply and ecosystem conservation. The Dujiangyan Irrigation System, an ancient yet highly effective hydraulic engineering project, continues to provide water resources for Chengdu and surrounding regions, holding significant historical and cultural value. Demographically and economically, Chengdu registered a permanent population of 15.982 million with an urbanization rate of 80.5%. As of early 2021, the city's gross domestic product reached 1,991.698 billion yuan, with per capita GDP increasing by 6.7% year-on-year, while the tertiary sector contributed 69.4% to the

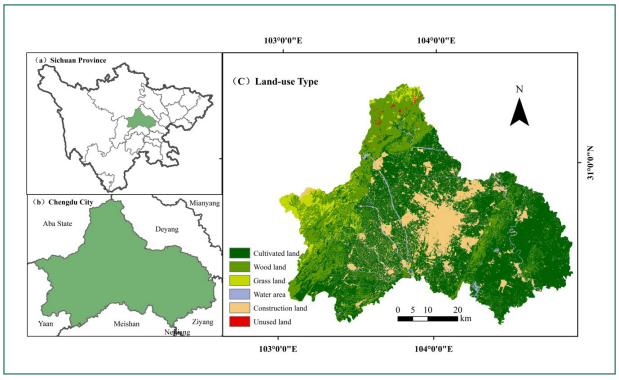

Figure 1 Spatial distribution of land use types in Chengdu

economic output. In terms of transportation and resource endowment, Chengdu possesses a comprehensive transportation network encompassing railways, highways, and aviation infrastructure, along with abundant natural gas reserves. Leveraging these advantages in economy, transportation, and resources, Chengdu has progressively evolved into a strategic growth hub in southwestern China and a nationally designated central megacity.

2. Data Sources

Informed by the identified characteristics from the research region, the data employed in this research primarily include land use datasets, natural condition parameters, and socioeconomic statistics. Detailed sources for all datasets are provided in Table 1. Physical and socio-economic factors primarily act as primary drivers of land use change for extracting transition rules in the FLUS model. Guided by the actual context of the research region and data accessibility, 14 influencing factors were selected, including distance to roads, distance to railways, distance to water area, annual precipitation, DEM, population density, GDP per unit area, and nighttime light index, among others. Transportation and water area data were processed by converting vector data into 30m×30m raster maps of driving factors. To enhance simulation accuracy and generate more realistic land use predictions, restricted zones were designated, including water-protected areas and nature reserves. All spatial datasets were uniformly processed in ArcGIS 10.2, undergoing resampling to a 30m×30m resolution, and all spatial data were uniformly projected using the WGS84 UTM Zone 48N coordinate framework.

Table 1 Data sources

Data Type	Data Name	Data Source
Land Use Data	Land Cover Data	https://www.resdc.cn/
Natural Condition Data	NDVI	https://www.resdc.cn/
	Soil Type	https://www.resdc.cn/
	Annual Average Temperature	https://www.resdc.cn/
	Annual Average Precipitation	https://www.resdc.cn/
	DEM	https://search.earthdata.nasa.gov/
	Slope	https://search.earthdata.nasa.gov/
	Aspect	https://search.earthdata.nasa.gov/
Socio-economic Data	Population Density	https://www.resdc.cn/
	GDP Per Unit Area	https://www.resdc.cn/
	Nighttime Light Data	https://www.resdc.cn/
	Distance to District/Town Centers	https://www.webmap.cn/
	Distance to Roads	https://www.openstreetmap.org/
	Distance to Railways	https://www.openstreetmap.org/
	Distance to Water Area (Rivers)	https://www.openstreetmap.org/
Panel Data	Economic Data for Agriculture, Forestry, and Fishing	《Chengdu Statistical Yearbook》
	Economic Data for the Three Major Grain Crops	《Chengdu Statistical Yearbook》, 《National Compilation of Cost-Benefit Data of Agricultural Products》

3. FLUS Model

The FLUS model employed in this study serves as an effective simulation tool for predicting future land use scenarios. By integrating Artificial Neural Network (ANN), System Dynamics (SD), and Cellular Automata (CA) technologies, it can address competitive land use transitions Process under multiple driving factors, thereby providing methodological support for subsequent simulation analyses. The model informed by regional land

utilization change regular and natural ecological development effects. It utilizes ANN to analyze various driving factors and yield suitability likelihood for different land utilization types. The SD module quantifies land utilization demands from a macro-perspective by measuring the influences of both socioeconomic development and natural conditions, while the CA module, through a dynamic adaptive inertial competition mechanism, addresses the spatial competition among multiple land-use types within complex systems. By configuring land use transition matrices and neighborhood factor weights, the FLUS model achieves high-precision spatiotemporal distribution simulations, with results closely aligned with actual land use change processes.

4. MOP Model

Considering the different emphases in urban development goals, four scenarios were established to predict the Spatial Configuration of Land Use in 2040: ND, END, ELD, and CD. The ND scenario simulates urban expansion under current policy frameworks without imposing additional constraints. This scenario requires identifying the optimal simulation model and time interval scale to maximize predictive accuracy, thereby establishing the baseline for calculating land use areas across different scenarios. For other scenario configurations, each must be paired with corresponding land use structure optimization schemes (Table 2), while incorporating measurements of both economic and ecological benefits. The END scenario determines the areal composition for six land use types by applying the principle of economic benefit maximization. The ELD scenario determines the areal composition for six land use types by applying the principle of ecological benefit maximization. The CD scenario represents a sustainable approach that harmonizes immediate advantages

Table 2 Constraints (hm^2)

Constraint Type	Constraint Conditions	Constraint Definition
Constraint on Total Land Area	$A = \sum_{i=1}^{6} X_i$	The total areas of the six land utilization types equals the combined area of Chengdu, 1433500.
Constraint on Cultivated Land Area	$593584.31 \leqslant X_1 \leqslant 791737.7$	Historical trend analysis indicates a persistent decrease in cultivated land area, with the projected change expected to be less pronounced than that observed in 2020. The lower bound was set at 20% below the ND scenario forecast, while the 2020 actual value served as the upper bound for regional projections.
Constraint on Wood Land Area X_1	$251516.33 \leqslant X_2 \leqslant 325199.37$	Historical data show a declining trend in total wood land area, with future changes expected to be more modest than those observed in 2020. The lower bound was defined as 20% below the ND scenario projection, while the 2020 actual value served as the upper bound for regional estimates.
Constraint on Forest Cover	$372710 \leqslant 0.46X_1+X_2+0.49X_3$	According to Chengdu's "Territorial Spatial Plan (2020-2035)", the forest coverage rate must reach at least 26% by 2035. This forest coverage constraint represents a crucial requirement for the Harmonious Sustainable Development. Within the land system, only cultivated land, wood land, and grass land qualify for meeting this constraint, with corresponding coefficients of 0.46, 1.00, and 0.49 respectively for calculating their contributions to forest coverage.
Constraint on Landscape Diversity	$54473 \leqslant X_3+X_6$	To preserve landscape diversity and accommodate urban expansion needs, as grass land and unused land are frequently converted for agricultural or urban development, their combined area shall be maintained at no less than 3.84% of the total land area by 2035.
Constraint on Water Area	$24623.61 \leqslant X_4$	Historical trend analysis indicates a continuous expansion of water area, with future changes expected to exceed the 2020 level. The actual 2020 value was set as the regional lower bound for projections.
Constraint on Construction Land	$229712.53 \leqslant X_5 \leqslant 342798.89$	Historical trend analysis reveals a consistent upward trajectory in construction land area, with projected future changes expected to exceed the 2020 level. The upper bound was established at 20% above the ND scenario forecast, while the actual 2020 value serves as the lower bound for regional projections.
Non-negative constraint on decision variables	$X_i \geqslant 0$, i=1～6	The non-negative nature of land area dictates that all corresponding decision variables in the study must assume values greater than or equal to zero.

with sustainable long-term gains, achieving equilibrium between economic and ecological objectives through optimized land use allocation. This scenario is realized by adjusting the areal composition of different land use categories, enabling comparative analysis across multiple scenarios.

1) Economic Benefit Objective Function

Leveraging data on the economic productivity of different land types (2000-2020), the economic efficiency coefficients for Chengdu in 2035 were projected using the GM(1,1) model, and the corresponding economic efficiency objective function was formulated. The economic productivity of various land categories within Chengdu was assigned corresponding industrial production values: cultivated land used planting industry data, wood land adopted forestry outputs, grass land utilized animal husbandry figures, water area employed fishery production data, while construction land incorporated the gross productivity of the secondary sector and tertiary Sector (Tang et al., 2022). Given the minimal and fragmented distribution of unused land in Chengdu, its economic benefits were excluded from the analysis.

$$\max f_1(x)=19.674x_1+2.144x_2+93.385x_3+27.504x_4+1749.315x_5+0x_6 \quad (1)$$

2) Ecological Benefit Objective Function

The core manifestation of ecological benefits lies in ecosystem service value (ESV), encompassing multiple categories such as regulatory, supportive, and cultural services. Costanza et al. (1997) provided a seminal reference for subsequent ecological benefit assessments by quantifying 17 ecosystem functions across 16 ecosystem types. Xie Gaodi (2015) subsequently adapted this classification system to align with China's specific ecological context. Multiple methodologies are currently available for assessing ESV, including

the physical quantity method, energy value analysis, shadow engineering approach, and travel cost method. This study employed the area-equivalent correction method to calculate ESV and formulate the ecological benefit objective function. The ESV was appropriately calibrated using the ratio of grain output per unit area between Sichuan Province and the national average, followed by the application of the GM(1,1) model to forecast Chengdu's ecological benefit coefficients for 2035.

$$\max f_2(x)=2.4872x_1+13.2562x_2+10.6646x_3+67.5091x_4+0.45x_5+0.1259x_6 \quad (2)$$

To verify the credibility of the adjusted economic efficiency coefficients, a sensitivity index was applied to examine the impact of coefficient variations for specific land types on the total ESV. By increasing and decreasing the ecological benefit coefficient of individual land types by 50%, the responsiveness of the total ESV to such parameter adjustments was evaluated. By adjusting the ecological benefit coefficients of various land types, the responsive sensitivity indices of different land categories toward ecological benefits can be calculated, with specific results presented in Table 3. All sensitivity indices recorded during the study period remained below 1, confirming the reliability of the coefficient adjustments and effectively ensuring the accuracy of land ecological benefit assessments. Among all

Table 3 Sensitivity index of different land use types

Year	Cultivated land	Wood land	Grass land	Water area	Construction land	Unused land
2000	0.2637	0.4866	0.0785	0.1711	0.0065	0.0001
2005	0.2569	0.4921	0.0792	0.1718	0.0080	0.0001
2010	0.2418	0.5063	0.0738	0.1781	0.0096	0.0001
2015	0.2381	0.5088	0.0743	0.1788	0.0108	0.0001
2020	0.2296	0.5025	0.0741	0.1938	0.0121	0.0001

land types, cultivated land and wood land demonstrated relatively higher sensitivity, indicating their more substantial influence on overall ecological benefit evaluation.

3) Objective Function for Balancing Economic and Ecological Benefits

By assigning different weights to ecological and economic benefits, this objective function enables the calculation of corresponding ecological and economic benefits of land use under varying weight allocations. Drawing on existing literature and applying the Pareto optimality strategy, the balancing act between ecological and economic objectives was analyzed by calculating the rate of ecological gain achieved per 1% reduction in economic benefits (i.e., the eco-economic conversion rate). This analysis ultimately determined that equal weighting of 0.5 for both dimensions yields the optimal land use structure.

$$\max\{f_1(x), f_2(x)\} \tag{3}$$

In the formula, x_1, x_2, x_3, x_4, x_5, x_6 represent cultivated land, wood land, grass land, water area, construction land, and unused land, respectively, measured in hectares (hm^2).

5. LER assess

1) Delineation of LER assess Units

When utilizing grid cells as assessment units and considering regional characteristics, the optimal grid size is typically determined as 2-5 times the average patch area within the region, based on principles of landscape ecology (Karimian et al., 2022). To further refine the grid dimensions, this study employed GS+ software to conduct semi-variogram fitting for the 2020 LER

Table 4 LER index semi-variance function model fitting results at different scales in 2020

Scale	C0	C+C0	C/(C+C0)	A/m	R^2	RSS
2km	2.23×10^{-4}	4.48×10^{-4}	0.501	46600	0.950	2.54×10^{-9}
3km	1.47×10^{-4}	3.47×10^{-4}	0.575	44600	0.919	3.90×10^{-9}
4km	1.36×10^{-4}	3.55×10^{-4}	0.617	47600	0.895	6.44×10^{-9}
5km	1.03×10^{-4}	3.07×10^{-4}	0.663	44500	0.936	3.05×10^{-9}

index at different spatial scales. The most suitable grid size was selected with reference to the coefficient of determination (R^2) and residual sum of squares (RSS) derived from the model fitting. When the fitting results show a high R^2 value coupled with a small residual RSS, it indicates superior fitting performance at the corresponding grid scale. According to the fitting outcomes presented in Table 4, the research area is partitioned into 2km ×2km LER grid cells using ArcGIS, generating a total of 3,825 assessment units. LER values for each unit were quantified using Fragstats 4.2 software. Subsequently, the geometric centroids of all risk units served as input parameters for the Kriging interpolation model.

2) Construction of the LER Index Model

Informed by existing studies and considering the actual conditions of Chengdu, a LER assessment model was constructed by integrating landscape type area proportion and landscape loss degree index. The landscape loss degree index is derived from the integration of the landscape vulnerability index and the landscape disturbance index. As a quantitative indicator, the LER index accurately characterizes the risk status of Chengdu's landscape ecosystem. With reference to existing LER classification methods and consideration of Chengdu's actual characteristics, the LER index was classified into five distinct risk tiers—low, relatively low, moderate, relatively high, and high—through the application of the natural breaks (Jenks) classification algorithm. This approach aims to precisely

represent the spatial pattern of LER, which is mathematically represented as:

$$ERI_{ki}=\sum_{i=1}^{m}\frac{A_{ki}}{A_k}R_i \quad (4)$$

In the formula, ERI_{ki} represents the LER index of landscape type i in evaluation grid cell k (where k = 1, 2, 3, ..., N); m denotes the total count of landscape types; A_k denotes the aggregate area of assessment grid cell k; A_{ki} represents the area of landscape type i within assessment grid cell k; R_i refers to the landscape loss degree index corresponding to landscape type i. A higher value of this index indicates a greater LER tier in the research area, while a lower value corresponds to reduced ecological risk.

6. Spatial Autocorrelation Analysis

Spatial autocorrelation measures the clustering patterns and dispersion degree of variables, comprising both global Moran's I and local Moran's I indices. The degree of geographical association of attributes within the study area was assessed using Global Moran's I. The statistic ranges from –1 to 1. Positive values indicate positive spatial autocorrelation, with higher values reflecting more pronounced spatial clustering. Conversely, negative values demonstrate dispersed spatial patterns. A value of 0 suggests the absence of significant spatial autocorrelation, representing a unpatterned geographical distribution. Local Moran's I is applied to identify how specific attributes cluster within limited spatial regions. A negative local Moran's I indicates negative spatial association, identifying areas where high and low values are adjacent between a spatial unit and its neighbors, reflecting significant spatial dissimilarity. Conversely, a positive local Moran's I indicates positive spatial autocorrelation, identifying areas of high-value or

low-value clustering, demonstrating low spatial variation among neighboring grid cells, and confirming the presence of spatial aggregation.

III. Results

1. Analysis of LER Dynamics

1) Analysis of Spatiotemporal Changes in LER

Between 2000 and 2020, Chengdu exhibited a notable trend of structural optimization in its LER. The average LER index decreased consistently from 0.0189 to 0.0171, indicating steady improvement in the overall ecological condition. The core driver of this improvement lies in the fundamental transformation of the risk level structure (Fig. 2). In 2000, the LER pattern was dominated by relatively high-risk levels, with nearly half the area classified as higher-risk. By 2020, the risk structure had shifted to one where medium-risk areas became predominant, forming a more stable, low-risk "spindle-shaped" structure characterized by a large middle and small extremes. Specifically, the area of low and medium-risk zones continued to expand, increasing by approximately 25%, while the area of high and higher-risk zones contracted significantly, decreasing by nearly 30%.

This structural transformation did not occur at a uniform pace. The most dramatic adjustments occurred between 2000 and 2005, primarily manifested as the expansion of medium-risk areas and the reduction of high-risk areas. Subsequently, the focus of risk level transition gradually shifted downward. By the 2015-2020 period, the significant contraction of high and higher-risk zones became the dominant force driving the overall risk "downward," signifying that the effects of Chengdu's ecological management efforts were most significant in the areas of highest risk.

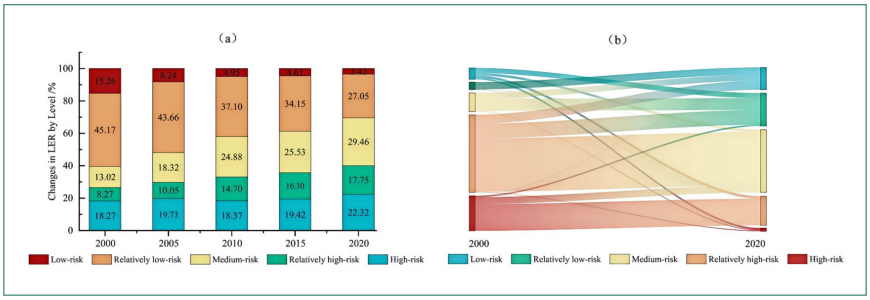

Figure 2 Change in LER in Chengdu

2) Analysis of LER Transition Changes

The transition matrix of LER grades (Fig. 3) corroborates the aforementioned overall risk reduction trend from a process-oriented perspective and reveals its underlying transformation mechanisms. Between 2000 and 2020, the evolution of LER in Chengdu demonstrated a high degree of orderliness and improvement-oriented transition.

Orderliness is reflected in the fact that risk grade transitions primarily occurred between adjacent levels, indicating that the evolution of LER is a relatively stable and gradual process rather than one characterized by abrupt, leapfrog changes.

Improvement-oriented transition is manifested as a distinct "downgrading"-dominated characteristic. The conversion from higher to lower risk zones accounted for an overwhelming proportion of the total transition area, constituting the core driver of optimization in the overall risk pattern. In contrast, reverse "upgrading" transitions were negligible (only 2.28%), further confirming the robustness of this improvement trend. Although a notable proportion of non-adjacent leapfrog transitions occurred in low-risk areas during 2005–2010, suggesting possible localized disturbances during this period, this episode did not alter the overarching two-decade trend of sustained and steady risk reduction.

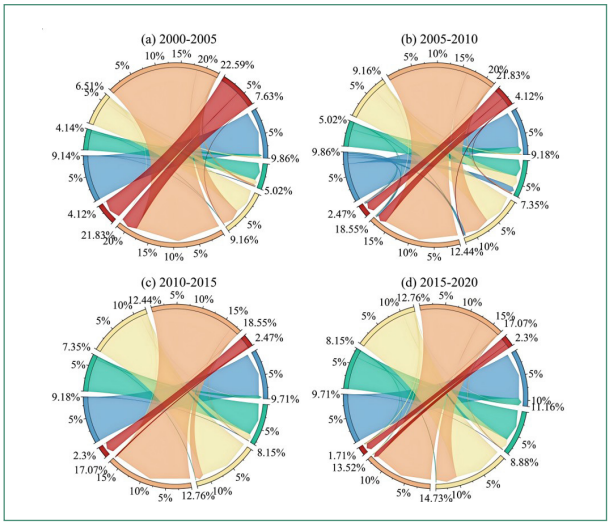

Figure 3 Transition of LER in Chengdu

2. Spatial Autocorrelation Analysis of LER

1) Global Spatial Autocorrelation Analysis

Global spatial autocorrelation analysis confirms a highly significant positive spatial correlation pattern in Chengdu's LER between 2000 and 2020. The global Moran's I indices for each year were accompanied by exceptionally high Z-scores and significance levels of $P < 0.001$ (Table 5), indicating that the spatially clustered patterns of LER were non-random and highly statistically significant.

However, the intensity of this spatial clustering demonstrates a clear and gradual weakening trend. Moran's I index decreased significantly from 0.654 in 2000 to 0.495 in 2020. This persistent decline suggests a weakening of the LER "club" effect in Chengdu, with its spatial distribution evolving from clearly clustered high-risk/low-risk blocks in the early period towards a more mixed and homogeneous pattern in later stages. This loosening of spatial dependency is associated with driving factors such as the

Table 5 Global Moran's I Analysis of LER

Year	Moran's I	Z	P
2000	0.654	79.365	0.001
2005	0.640	77.679	0.001
2010	0.517	62.722	0.001
2015	0.513	63.240	0.001
2020	0.495	60.238	0.001

diversification of land use patterns resulting from urbanization and the decentralized implementation of ecological policies.

2) Local Spatial Autocorrelation Analysis

LISA cluster analysis (Fig. 4) reveals that the local spatial correlation of LER in Chengdu presents a significant "bipolar clustering" pattern, dominated by "High-High" and "Low-Low" clusters, while transitional outliers ("Low-High", "High-Low" clusters) account for an extremely low proportion (approximately 1%), indicating that high-risk and low-risk areas are internally highly continuous yet lack buffers between each other. The "High-High" clusters, acting as key risk sources, are distributed in continuous patches, showing a fluctuating downward trend in coverage rate, primarily located in water bodies and cultivated areas susceptible to human disturbance, with poor landscape

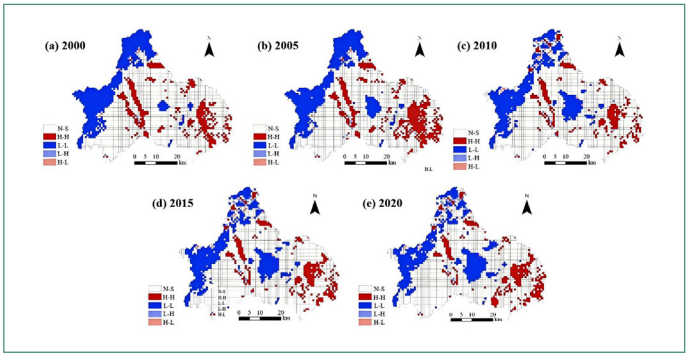

Figure 4 LISA Cluster Analysis of LER

stability. The “Low-Low” clusters form the core ecological barriers, concentrated in the central-western part, with their coverage rate decreasing from 21.49% to 19.03%, suggesting that the superior ecological base is under pressure. The scarcity of outliers further increases the potential risk of confrontation between high and low-risk zones. Therefore, ecological risk management should adhere to the strategy of “consolidating barriers and treating sources”, focusing on targeted governance in high-risk cluster areas while strictly protecting the western low-risk cluster areas to block their spatial radiation effects.

3. Analysis of Drives of LER

1) Factor Detection

Geodetector analysis indicates that natural factors are the dominant drivers of the spatial heterogeneity of LER in Chengdu. In the single-factor detection, the p-values of all driving factors passed the significance test ($p=0.001$) (Table 6). Mean annual temperature was the most critical factor affecting risk heterogeneity ($q=0.284$), followed by DEM ($q=0.275$), NDVI ($q=0.238$), and slope ($q=0.198$). In contrast, socioeconomic and accessibility factors exhibited weaker explanatory power ($q<0.1$), indicating that the LER pattern is primarily constrained by the underlying natural conditions.

2) Interfactor Interactions Analysis

This dominant pattern exhibited dynamic evolutionary characteristics from 2000 to 2020 (Fig. 5). In 2000, it was primarily led by NDVI and mean annual temperature. By 2020, the influence of DEM and mean annual temperature had significantly strengthened, with their explanatory powers both exceeding 0.45, reflecting that the constraining effects of topography and climate on the landscape pattern have become increasingly prominent

Table 6 Analysis of LER Drivers in Chengdu

Factor Layer	Indicator Layer	No.	2000	2005	2010	2015	2020	Rank
Natural Factors	DEM	X1	0.1389	0.1469	0.2022	0.4053	0.4793	2
	Slope	X2	0.0759	0.1044	0.127	0.3135	0.3696	4
	Aspect	X3	0.0055	0.0061	0.0081	0.0091	0.0143	14
	Soil Type	X4	0.0258	0.0226	0.0559	0.1826	0.2203	8
	NDVI	X5	0.2052	0.2067	0.2058	0.2747	0.2953	3
	Annual Average Precipitation	X6	0.0397	0.0543	0.0551	0.1699	0.1892	7
	Annual Average Temperature	X7	0.1881	0.2286	0.1441	0.3988	0.4611	1
Regional Accessibility	Distance to District/ Town Centers	X8	0.0382	0.041	0.0415	0.1051	0.1355	11
	Distance to Roads	X9	0.0221	0.0234	0.0212	0.0834	0.1044	12
	Distance to Railways	X10	0.0626	0.0795	0.094	0.2328	0.2778	5
	Distance to Water Area	X11	0.0075	0.0166	0.0191	0.0723	0.1051	13
Socio-economic Factors	Population Density	X12	0.0955	0.0709	0.0613	0.0888	0.1201	10
	GDP Per Unit Area	X13	0.1066	0.0791	0.0964	0.0543	0.1213	9
	Nighttime Light Index	X14	0.1003	0.09	0.0876	0.089	0.1535	6

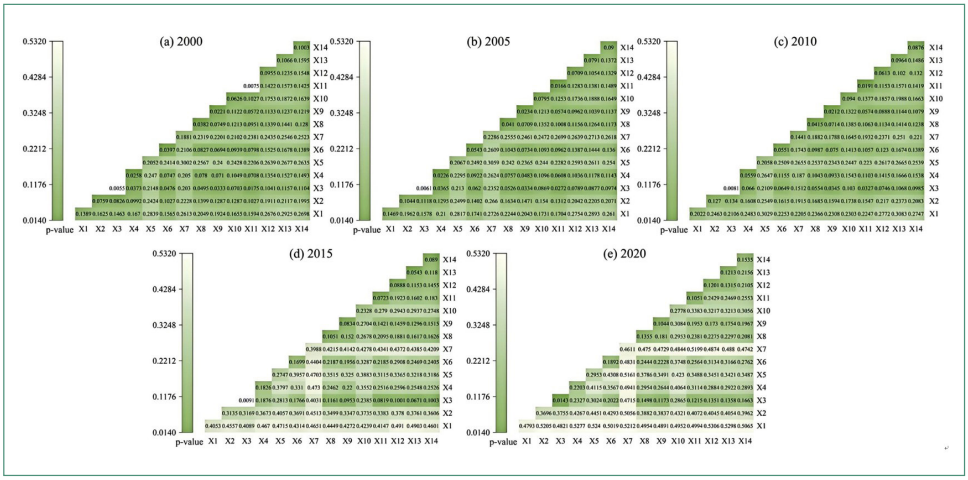

Figure 5 Interaction results of driving factors for LER in Chengdu

alongside the intensification of human activities. Interaction detection further revealed that all factor pairs exhibited a two-factor enhancement effect, with significant interactions among natural factors. The interactive explanatory power of combinations like DEM & mean annual temperature and DEM & NDVI exceeded 50% in 2020, demonstrating that LER results from the nonlinear coupling of multiple natural and socioeconomic elements. This finding emphasizes that future ecological risk management should focus on the synergistic enhancement effects produced by the combination of key natural factors in different geographical contexts.

4. Multi-Scenario Land Use Simulation and Prediction

1) Accuracy Validation Multi-Scenario Land Use Models

To ensure the reliability of future scenario simulations, this study used the actual land use data from 2020 as a benchmark and systematically compared the simulation performance under different parameters and data configurations through the control variable method, aiming to select the most robust simulation path for the 2035 prediction. Model accuracy was jointly evaluated by the overall accuracy and the Kappa coefficient. Among these, the Kappa coefficient is regarded as a superior indicator for measuring the consistency between simulation results and real data because it can effectively eliminate the interference of random classification; its value is higher, indicating the model's simulation performance is superior.

(1) Comparing the Simulation Accuracy of Two Models

To enhance the improvement of simulation results, two models - both the PLUS and FLUS models - were selected to simulate the land use configuration of 2020 (Figure 6). Model accuracy validation showed that the evaluation results showed the PLUS model produced a Kappa index of

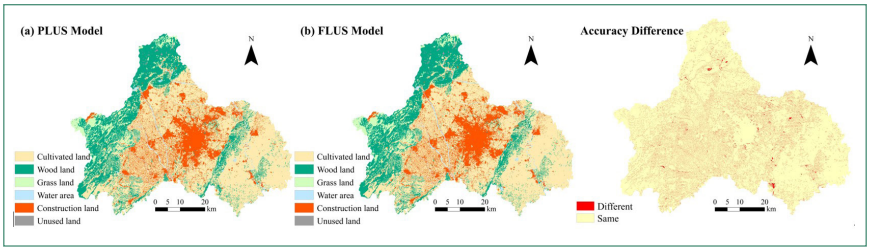

Figure 6 Variations in model accuracy in Chengdu

81% with 88.3% accuracy; the FLUS model recorded significantly higher results at 87% Kappa and 92% accuracy. The comparative results indicate that the FLUS model demonstrates superior accuracy in simulating land use evolution.

(2) Comparing Simulation Accuracy Across Different Temporal Spans

To improve the accuracy of the simulation results, two temporal spans - a ten-year interval (2010-2020) and a five-year interval (2015-2020) - were selected to simulate the land use pattern of 2020 (Fig. 7). Model accuracy validation showed that the simulation using the five-year interval produced a Kappa index of 86.98% with 92% accuracy, while the simulation using the ten-year interval produced a Kappa index of 79.72% with87.51%accuracy. The comparative results indicate that shorter temporal spans demonstrate superior accuracy in simulating land use evolution.

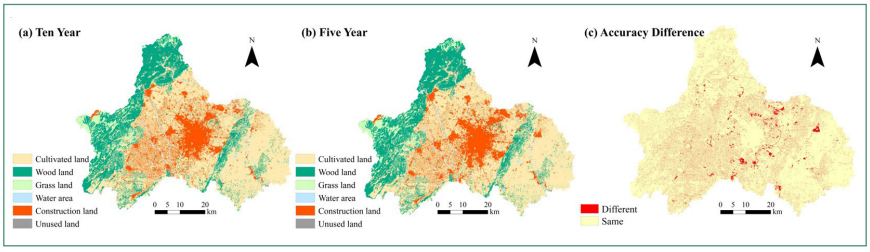

Figure 7 Accuracy differences across various time spans in Chengdu

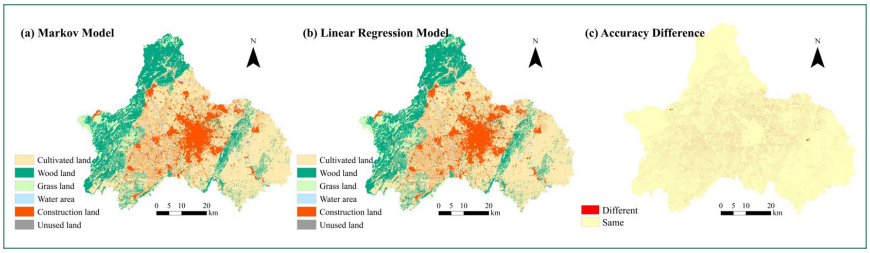

Figure 8 Differences in prediction method accuracy in Chengdu

(3) Comparing the Simulation Accuracy of Different Quantity Prediction Methods

To enhance the accuracy of the simulation results, two quantity prediction methods - both the Markov and Linear Regression models - were selected to simulate the land use pattern of 2020 (Fig. 8). Model accuracy validation showed that simulation using the Markov model produced a Kappa index of 81.51% with 88.63% accuracy, while simulation using the Linear Regression model produced a Kappa index of 81.39% with88.55%accuracy. The comparative results indicate that the Markov model demonstrates superior accuracy in simulating land use evolution.

(4) Accuracy Validation of the 2020 Projections

The 2020 land use configuration of Chengdu was simulated using land use/cover data from 2015-2020 and 14 corresponding drives. The simulated

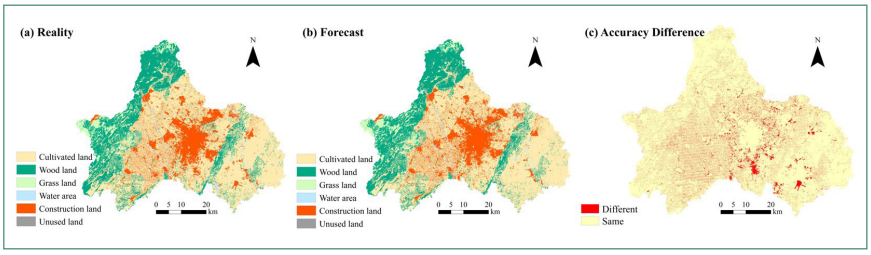

Figure 9 Accuracy variations in Chengdu

outputs were next spatially compared with the actual distribution (Fig. 9). The FLUS model demonstrated high simulation accuracy, with most land type simulation accuracies exceeding 90%. Only the accuracies for water bodies and construction land were slightly lower, at 85.56% and 82.92%, respectively.

2) Multi-Scenario Landscape Type Change Analysis for 2035

The multi-scenario land use simulation results (Table 7, Fig. 10) profoundly reveal the potential pathways of Chengdu's landscape pattern in 2035 under different policy orientations. The macro-scale pattern of the "Northeastern Ecological Conservation Area" and the "Central-Western Urban-Rural Development Area" remains stable across all scenarios, but their evolution patterns and ecological impacts are fundamentally different.

Both the ND and END scenarios predict the continued squeezing of ecological space by high-intensity development. Under the ND scenario, the disorderly expansion of construction land directly encroaches on a large amount of high-quality cultivated land, and further forces marginal woodland to be converted into cultivated land, showing the inertial pressure of sprawling development. The END scenario pushes this development intensity to the extreme, with the area of cultivated land sharply decreasing by 8%. The rate and scale of this loss far exceed those in the ND scenario, clearly revealing the enormous ecological cost inevitably brought by solely pursuing economic growth. In contrast, the ELD and CD scenarios demonstrate the optimizing effect of effective policy intervention on spatial order. The ELD scenario, by strictly restricting the expansion of construction land, maximally preserves the scale and distribution of ecological lands such as woodland and grassland, proving that controlling development intensity at the source is key to maintaining the ecological base. The CD scenario reflects a more refined regulatory logic. Although

its direction of change is similar to the ND scenario, the magnitude of change for all key land types (e.g., cultivated land loss, construction land expansion) is effectively curbed. This indicates that, while acknowledging development needs, it is entirely possible to significantly slow the degradation rate of ecological land and rebalance the relationship between development and protection through strong cultivated land protection and construction land control.

In summary, the simulations clearly present the core trade-offs under different pathways: the END scenario centrally reflects the spatial demands of economic development, at the cost of rapid cultivated land loss and ecological squeezing; the ELD scenario is the most thorough in ecological preservation, imposing the strictest limits on construction demand; the CD scenario finds a feasible path that balances economy and ecology, whose outcomes are highly aligned with the orientation of regional sustainable development, providing crucial scientific evidence for decision-makers. Unused land did not undergo significant changes in any scenario due to its

Table 7 Area and changes of landscape types under multi-scenario in Chengdu (km, %)

Year	Unit	Cultivated land	Wood land	Grass land	Water area	Construction land	Unused land
2020	area	7917.70	3252.40	595.30	245.59	2297.58	26.43
	Percentage	55.23	22.69	4.15	1.71	16.03	0.19
ND	area	7493.02	3170.57	596.68	284.38	2763.92	26.42
	Percentage	52.27	22.12	4.16	1.98	19.28	0.18
END	area	7377.07	3389.19	625.01	272.91	2643.43	27.38
	Percentage	51.46	23.64	4.36	1.90	18.44	0.19
ELD	area	7535.73	3430.18	615.16	306.87	2420.59	26.48
	Percentage	52.57	23.93	4.29	2.14	16.89	0.18
CD	area	7466.10	3239.99	606.98	279.44	2716.42	26.07
	Percentage	52.08	22.60	4.23	1.95	18.95	0.18

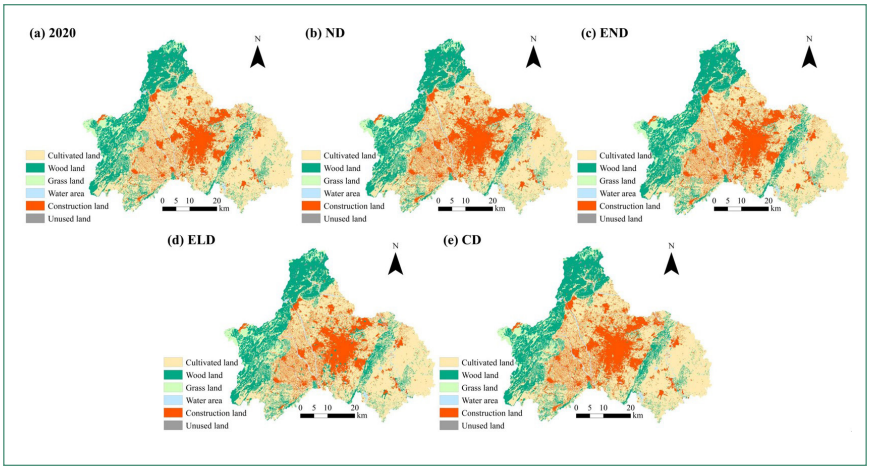

Figure 10 Spatial distribution of landscape types under multi-scenarios in Chengdu

low baseline proportion.

3) Analysis of Multi-Scenario LER Changes in 2035

The simulation of future LER shows that the spatial pattern of risk in Chengdu in 2035 maintains a high degree of inheritance from the historical distribution under different scenarios (Figure 11, Figure 12). However, the average risk level varies depending on policy choices, showing subtle yet

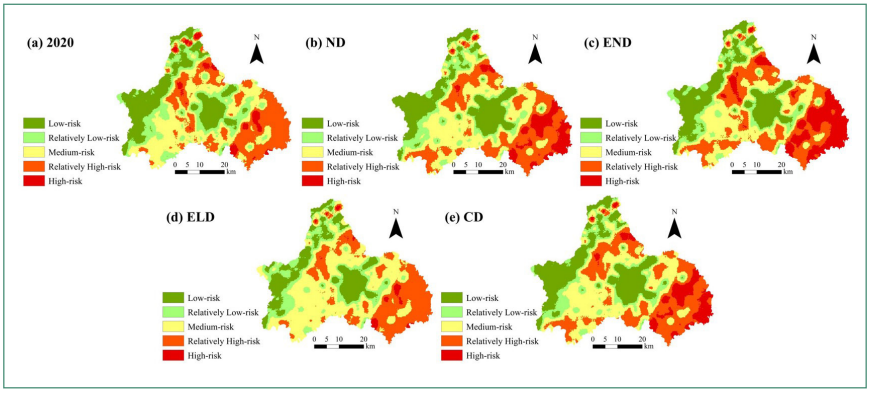

Figure 11 Spatial distribution of LER under multi-scenarios in Chengdu

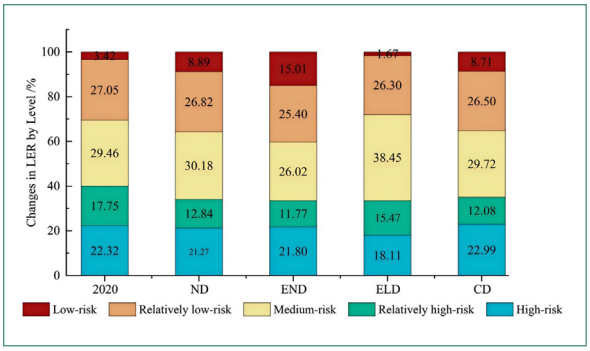

Figure 12 LER in Chengdu: A Analysis across Multiple Scenarios

critical differences. The average LER indices for all four scenarios remain above 0.020, belonging to the medium-risk category, but this does not mean that policies are ineffective.

Based on the simulation of future LER, we conducted a comparative analysis of the risk level pattern in Chengdu for the year 2035 under four development scenarios (Fig. 13). The results show that different policy pathways will have distinct impacts on regional ecological security.

Under the ND scenario, the LER pattern remains relatively stable, with limited changes in the area of each risk level. However, the risk structure shows a slight "upgrading trend", specifically manifested as the transformation of low and relatively low-risk areas into adjacent higher levels, resulting in a significant increase of 783.17 km^2 in high-risk areas. This indicates that even by maintaining the current development trajectory, regional ecological pressure will continue to accumulate. While no fundamental deterioration of the risk pattern occurs, there is also a lack of momentum for improvement.

Under the END scenario, the risk pattern undergoes drastic restructuring. Large-scale transfers between levels towards higher risk levels occur, ultimately causing the high-risk area to surge to 1660.86 km^2, more than doubling compared to the ND scenario. The significant diffusion and

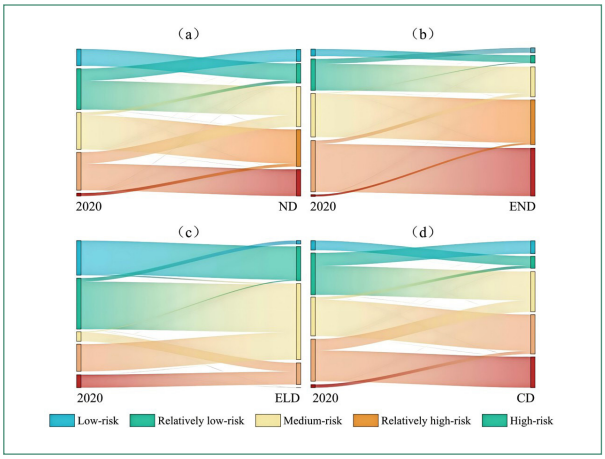

Figure 13 Transition of LER under multi-scenarios in Chengdu

intensification of risk clearly warn that an economic development model achieved at the expense of ecology will pose a serious threat to regional ecological security. In contrast, the ELD scenario exhibits an ideal "risk convergence" pattern. Risk levels show a systematic, bidirectional trend of "converging towards the middle", forming a complete hierarchical optimization pathway. The result is a substantial reduction of 1009.29 km^2 in the high-risk area, accompanied by a corresponding expansion of the medium-risk area. This pattern eliminates extremely high risk and avoids excessive risk aggregation, signifying an ecosystem in a controllable and benign development state. The risk pattern under the CD scenario is the most complex, with its risk level situated between the ND and ELD scenarios. This scenario exhibits the coexistence of high-risk area expansion and relatively low-risk area reduction, indicating that its regulatory mechanism has not yet fully contained the localized deterioration of risk. This result suggests that achieving coordinated development requires more refined spatial management strategies, rather than a simple compromise.

Overall, the simulation results from the different scenarios clearly reveal the causal relationship between policy choices and ecological consequences,

providing clear scientific evidence for regional sustainable development decision-making.

IV. Discussion

1. Scenario-Based Evolution of LER

The different scenarios' simulation results reveal significant differences in LER patterns in Chengdu under different development policy orientations. Under both the ND and END scenarios, the loss of cultivated land is a direct consequence of the haphazard spatial sprawl of construction land and ecological land, driving an increase in the mean LER index and triggering intense transitions toward higher risk levels. The expansion of high-risk areas demonstrates a clear trend of risk structure shifting toward higher grades. Without effective spatial regulation, the current development model will result in continued decline in ecosystem stability and further intensification of LER.

Under the ELD Scenario, the stringent control of construction land expansion and effective maintenance of ecological land scale have resulted in a marked contraction of high-risk zones, confirming that robust ecological protection is the most effective approach to enhancing regional ecological security. In contrast, the simulation results of the CD Scenario fall short of expectations, with the overall risk level situated between the ND and ELD scenarios, and a substantial expansion of high-risk areas still observed. This indicates that, under current development conditions, if coordination relies solely on macro-level balanced regulation without rigid constraints on key ecological elements, the diffuse nature of objectives in so-called "coordinated development" proves difficult to effectively curb ecological

degradation and fails to achieve substantial improvement in ecological environmental quality.

2. Recommendations for Future Development

Based on the spatiotemporal evolution, driving mechanisms, and multi-scenario simulation results of LER, the following recommendations are proposed for the sustainable development of Chengdu:

First, Implement Differentiated Ecological Management Strategies. Delineate key control zones based on spatial autocorrelation analysis, specifically targeting "high-high" risk clusters in ecologically sensitive zones like water areas and cultivated land ecotones. In these zones, establish ecological buffer strips and promote agroecological practices to mitigate the risk of radiation effects. For medium- to high-risk cultivated areas, strictly enforce cropland protection policies and advance the development of high-standard cultivated land to maintain the stability of agricultural ecosystems.

Second, Construct a Comprehensive Ecological Security Pattern. Stringently protect the ecological barrier functions of the western "low-low" clusters by enhancing forest conservation and biodiversity maintenance. Advance the "Park City" initiative by improving ecological corridor networks to enhance intra-urban ecological connectivity, and establish a coordinated urban-rural ecological security system.

Third, establish a Long-term Monitoring and Planning-Oriented Mechanism. Develop a dynamic LER monitoring and early-warning system, with a specific focus on areas experiencing anomalous risk level transitions, to facilitate a shift from reactive remediation to proactive regulation. Ensure that territorial spatial planning fully accounts for the interactive effects of natural and socio-economic factors. By implementing scientifically informed spatial regulations, composite ecological risks can be mitigated, thereby

safeguarding the sustainable development of regional ecological security.

3. Limitations and Future Directions

The study has several limitations and constraints.

First, the landscape vulnerability weighting based on expert experience involves a degree of subjectivity. To test the robustness of the conclusions, the vulnerability index of construction land was increased from 1 to 6, substantially raising its landscape loss degree from 0.0064 to 0.2058. However, the sensitivity analysis results show that while the total area of high-risk regions and the significance of the spatial pattern changed, the two core conclusions—that the ELD scenario is the most effective path for risk control and that the CD scenario faces management challenges—remain valid. This demonstrates that the main findings of this study possess a certain robustness to the weight assignments. However, adopting objective weighting methods based on ecosystem service flows is a direction for improving assessment accuracy in future research.

Second, the choice of drivers was governed by the availability of data, leading to the exclusion of several potential determinants, including governmental policy interventions, socioeconomic fluctuations, and natural disaster events. This analysis was limited to fourteen quantifiable factors, potentially creating deviations between the projected scenarios and real-world ecological outcomes.

Third, the 30-meter resolution land data used in this study, while suitable for regional-scale analysis, struggles to precisely capture fine-grained ecological elements within the city, such as pocket parks, small green belts, and narrow river corridors. This leads to a systematic deviation in the assessment of LER within highly fragmented urban built-up areas, making it impossible to accurately quantify the actual contribution of fine-scale

ecological units in reducing local risk.

Fourth, in conducting the LER assessment, the study area was divided into 2 km × 2 km assessment units. The Kriging interpolation process for areas with irregular edges or where assessment center points fell outside the study area may have introduced some degree of error. Future studies could benefit from optimizing the spatial unit division scheme or employing alternative interpolation methods to minimize such potential inaccuracies.

Fifth, this study reveals a key policy dilemma. Although the MOP model indicates that a 0.5:0.5 weighting is theoretically the Pareto-optimal solution with the highest eco-economic conversion efficiency, the CD scenario simulated based on this, in practice, failed to effectively curb the expansion of high-risk areas. This "coordination failure" phenomenon profoundly reveals the gap between theoretical optimum and spatial implementation. In plain cities with significant ecological risk heterogeneity, homogeneous weight allocation cannot form effective constraints in critical locations. When regional development pressure approaches the ecological critical point, any "coordination" scheme lacking rigid spatial bottom lines as a precondition struggles to counteract the powerful inertia of economic development. Therefore, achieving coordinated development must go beyond macro-level weight balancing. It is necessary to transform identified key areas, such as "High-High" risk zones, into supplementary spatial rules that must be strictly enforced as peripheral extensions of the ecological protection redline. Only through precise, "one policy per parcel" management can the goals be achieved in practice.

V. Conclusions

This study systematically analyzed the evolution patterns of LER in

Chengdu from 2000 to 2035, yielding the following core conclusions:

First, in terms of temporal evolution, the LER in Chengdu exhibited structural improvement during 2000-2020. The average risk index continuously decreased, and the risk pattern achieved an optimized transformation from being dominated by relatively high-risk levels to being primarily composed of medium-risk levels. The transfer of risk levels was dominated by the "downgrading" from higher to lower risk levels, clearly revealing a positive development trend in the regional landscape ecological environment.

Second, in terms of spatial pattern, the risk distribution demonstrated stable spatial agglomeration and dynamic agglomeration intensity. The "High-High" and "Low-Low" risk agglomeration areas constitute the basic spatial skeleton of the regional ecological security pattern, highly coinciding with the ecologically sensitive zones in the plain hinterland and the ecological barrier in the western mountainous area, respectively. Meanwhile, fluctuations in the global agglomeration intensity suggest that its spatial structure is undergoing dynamic reorganization.

Third, regarding the driving mechanism, natural background conditions are the dominant factor in risk spatial heterogeneity, with mean annual temperature and DEM being the core driving factors. However, factor interaction detection reveals that LER is ultimately shaped by the nonlinear coupling of the natural-socioeconomic system. The interactive explanatory power of DEM and socioeconomic factors exceeds 50%, highlighting the profound impact of human activities on altering natural patterns.

Fourth, regarding future scenarios, the multi-scenario simulations provide clear warnings and guidance for policy choices. The ELD scenario is the most effective pathway for achieving fundamental optimization of ecological risk; whereas the CD scenario demonstrates the feasibility of balancing development needs with ecological protection, but its success highly

depends on precise ecological spatial management control. The research indicates that deeply integrating the ecology-priority principle into territorial spatial planning is key to ensuring sustainable urban development.

Submitted: October 14, 2025 | Revised: November 12, 2025 | Accepted: December 2, 2025

References

Hamad, R., H. Balzter, and K. Kolo. 2018. "Predicting Land Use/Land Cover Changes Using a CA-Markov Model under Two Different Scenarios." *Sustainability* 10(10): 3421.

Luo, G., C. Yin, X. Chen, W. Xu, and L. Lu. 2010. "Combining System Dynamic Model and CLUE-S Model to Improve Land Use Scenario Analyses at Regional Scale: A Case Study of Sangong watershed in Xinjiang, China." *Ecological Complexity* 7(2): 198-207.

Liu, P., Y. Hu, and W. Jia. 2021. "Land Use Optimization Research Based on FLUS Model and Ecosystem Services-Setting Jinan City as an Example." *Urban Climate* 40: 100984.

Guo, P., H. Wang, F. Qin, C. Miao, and F. Zhang. 2023. "Coupled MOP and PLUS-SA Model Research on Land Use Scenario Simulations in Zhengzhou Metropolitan Area, Central China." *Remote Sensing* 15(15): 3762.

Tang, H., B. Zhang, D. Ju, and A. Zhang. 2022. "Land Use Optimization Allocation in National Central Cities under Ecological-economic Trade-offs: A Case Study of Wuhan City." *Research of Soil and Water Conservation* 29(6): 416-424.

Costanza, R., R. d'Arge, R. de Groot, et al. 1997. "The Value of the World's Ecosystem Services and Natural Capital." *Nature* 387(6630): 253-260.

Xie, G., C. Zhang, L. Zhang, W. Chen, and S. Li. 2015. "Improvement of the Ecosystem Service Value Method Based on Unit Area Value Equivalent Factor." *Journal of Natural Resources* 30(8): 1243-1254.

Karimian, H., W. Zou, Y. Chen, J. Xia, and Z. Wang. 2022. "Landscape Ecological

Risk Assessment and Driving Factor Analysis in Dongjiang River Watershed." *Chemosphere* 307(Part 3): 135835.